ARTICLE

Highly flexible and accurate serial picoinjection in droplets by combined pressure and flow rate control

Received 00th January 20xx,
Accepted 00th January 20xx

DOI: 10.1039/x0xx00000x

Jolien Breukers,[a] Hannah Op de Beeck[a], Iene Rutten[a], Montserrat López Fernández[b,c,d], Sven Eyckerman[c,d] and Jeroen Lammertyn*[a]

Picoinjection is a robust method for reagent addition into microfluidic droplets and has enabled the implementation of numerous multistep droplet assays. Although serial picoinjectors allow to screen many conditions in one run by injecting different combinations of reagents, their use is limited because it is complex to accurately control each injector independently. Here, we present a novel method for flexible, individual picoinjector control that allows to inject a predefined range of volumes by controlling the flow rate of the injector as well as turning off injection by setting the equilibrium pressure, which resulted in a stable interface of the injector liquid with the main microfluidic channel. Robust setting of the equilibrium pressure of an injector was achieved by applying accurate ($R^2 > 0.94$) linear models between the injector and oil pressure in real-time. To illustrate the flexibility of this method, we performed several proof-of-concepts using 1, 2 or 3 picoinjectors loaded with fluorescent dyes. We successfully demonstrated picoinjection approaches using time-invariant settings, in which an injector setting was applied for prolonged times, and time-variant picoinjection, in which the injector settings were continuously varied in order to sweep the injected volumes, both resulting in monodisperse (CV < 3.4%) droplet libraries with different but reproducible fluorescent intensities. To illustrate the potential of the technology for fast compound concentration screenings, we studied the effect of a concentration range of a detergent on single-cell lysis. We anticipate that this robust and versatile methodology will make the serial picoinjection technology more accessible to researchers, allowing its wide implementation in numerous life science applications.

1. Introduction

Droplet microfluidics has become an important tool for numerous physical and life science applications(1–8), as it enables the miniaturization and high-throughput parallelization of chemical and biological assays by encapsulating reagents in femto- to microliter sized droplets at kHz or even MHz rates(9,10). Over the past years, multistep protocols with increasing complexity have been implemented into droplets thanks to the development of droplet manipulation techniques such as droplet sorting(11,12), splitting(13,14), fusion(15,16) and picoinjection(17,18). The latter is a robust method for reagent addition in which liquid in a side-channel is pressurized and consequently merges with passing droplets in the main channel, mostly under influence of an electric field(17). Picoinjection has found numerous applications in multistep reactions including directed evolution(5,19,20), multiplexed characterization of enzyme activity(2,21,22), identification and isolation of microorganisms with desired activity(23–26), single-cell identification through RT-PCR(27) and the synthesis of crystals(28,29), nanoparticles(29) and microgel beads(30).

Whereas single picoinjectors have been widely implemented, multiple picoinjectors in series are only rarely described(2,17,18). Nevertheless, serial picoinjection enables combinatorial reagent addition into the individual droplets, allowing to screen many conditions in one experimental run(2). However, current methods for serial picoinjection do not allow full control over each separate injector, limiting their widespread application. More specifically, to generate a higher impact for the serial picoinjection technology, it should be possible to choose the injected volume by each picoinjector independently, as well as to turn off each injector separately.

In existing methods, either the pressure or the flow rate of the picoinjector liquid is controlled. In systems with flow rate control, e.g., by the use of syringe pumps, it is straightforward to vary the injected volume by adapting the injector flow rate(22,28). However, it is nearly impossible to rapidly and completely stop the flow in small microfluidic channels by setting the flow rate to zero, impairing to robustly switch off an individual injector. For example, in a system with 3 serial injectors, in which the flow rates of the injectors were fixed at a low value and electrodes were turned off to stop injection, the deactivated injectors still occasionally formed droplets into the main channel due to the long and erratic pressure equilibration of the syringe pumps(2). Additionally, it was not demonstrated

[a] Department of Biosystems, Biosensors group, KU Leuven, Leuven 3001, Belgium. E-mail: jeroen.lammertyn@kuleuven.be
[b] Confo Therapeutics, Technologiepark-Zwijnaarde 30, Ghent 9052, Belgium.
[c] Center for Medical Biotechnology, VIB-Ghent University, Technologiepark-Zwijnaarde 75, Ghent 9052, Belgium.
[d] Department of Biomolecular Medicine, Ghent University, Technologiepark-Zwijnaarde 75, Ghent 9052, Belgium.
†Electronic Supplementary Information (ESI) available: [details of any supplementary information available should be included here]. See DOI: 10.1039/x0xx00000x

that the volume added by each picoinjector could be varied independently in this 3-injector system.

Switching off the injection without the formation of droplets is theoretically more straightforward when relying on pressure control. In the first report on picoinjection by Abate *et al.*(17), the pressure of the injector liquid was controlled at an equilibrium pressure, at which the injector liquid formed a stable interface with the oil in the main channel, and thus did not retract back into the injector channel nor formed droplets into the main channel. The pressure range at which an equilibrium state is achieved, is determined by the Laplace pressure, which is the pressure difference between the injector liquid and the main channel(17,18). When pressurizing the injector within the range for equilibrium, injection was turned on and off by respectively activating and deactivating the electrodes, and it was observed that the injected volume was linearly correlated with the applied pressure(17). Furthermore, a system with 3 injectors was shown in which one of the injectors was actuated while the others were deactivated. However, it was not demonstrated that the injected volume of the serial injectors could be varied or that multiple injectors could be used simultaneously. Additionally, in another study, it was observed that pressure fluctuations occurred in the main channel, which influenced the range for the equilibrium pressure and consequently resulted in unstable picoinjection(18). To tackle this problem, a pressure stabilizer was implemented before the injector to reduce the pressure instabilities, and a proof-of-concept study was performed with 2 injectors in series(18). Although this approach allowed to robustly switch off a picoinjector, the drawbacks of this system were that the injected volume depended on the initial droplet size, and that the injected volume could not be varied for both injectors independently.

As such, none of the existing serial picoinjection methodologies allows to vary the injected volume by each independent injector, as well as to robustly turn off one or more picoinjectors, which prevents accurate combinatorial injection of reagents at different concentrations. In this work, we aim to push the serial picoinjection technology to its full potential by developing a robust methodology for flexible control of separate picoinjectors in series, ultimately allowing to choose the injected volume by each injector at every point in time. To achieve this, we combine flow rate and pressure control to benefit from the strengths of both methods. More specifically, flow rate control is used when an injector is turned on to be able to accurately vary the injected volume, and pressure control is used when an injector is turned off. Here, pressure fluctuations in the main channel are taken into account by constructing a linear model between the equilibrium pressure of each injector and the oil pressure, based on which the injector pressure is adjusted in real-time. We first describe the concept of the method and the required set-up in more detail, after which we elaborate on the calibration of the equilibrium pressure models for the injectors. To illustrate the flexibility of this method, we perform several proof-of-concepts by injecting fluorescent dyes into droplets using single injectors as well as using 2 and 3 injectors in series. We demonstrate concepts using time-invariant picoinjector settings, i.e., in which certain injector settings are applied for a fixed time period, and droplets for each setting are collected in separate reservoirs, as well as for a novel picoinjection concept using time-variant settings, i.e., in which the injector settings are varied within a certain time frame to allow sweeping of the added volumes and thus generate a pooled droplet library with different injected volumes. Lastly, we show the potential of the technology for compound concentration screenings by injecting a detergent to droplets loaded with single human cells, thereby determining the required detergent concentration to achieve lysis of the cellular membrane and/or nucleus.

2. Materials and methods

2.1. Reagents and materials

SU-8 2025 was obtained from Chimie tech services (Antony, France) and 3-inch silicon wafers were purchased from Microchemicals GmbH (Ulm, Germany). Sigma Aldrich (Machelen, Belgium) was the supplier for propylene glycol methyl ether acetate (PGMEA), glycerol, phosphate buffered saline (PBS), trichloro(1H,1H,2H,2H-perfluorooctyl)silane, CHAPS hydrate and fluorescein sodium salt. Polydimethylsiloxane (PDMS) was bought as DC Sylgard 184 elastomer from Farnell (Grâce-Hollogne, Belgium). ThermoFisher Scientific (Waltham, MA, USA) supplied Alexa Fluor 350, Alexa Fluor 568, 0.05% Trypsin-EDTA, McCoy's 5a Medium, fetal bovine serum (FBS), Penicillin-Streptomycin (10,000 U/mL), Dulbecco's PBS (DPBS) and microfluidic tubing with inner diameter of 0.56 mm and outer diameter of 1.07 mm. KOVA glasstic slides with counting grids and 1 mL plastic syringes were purchased from VWR (Leuven, Belgium), and Sterican needles with 0.60 mm external diameter and calcium soda glass slides of 1 mm thickness were obtained from Carl Roth Gmbh (Karlsruhe, Germany). Biopsy punches of 1 mm diameter were acquired from BAP Medical B.V. (Apeldoorn, Netherlands) and microfluidic reservoirs for PDMS chip (XXS) were purchased from Darwin microfluidics (Paris, France). HCT116 cells (ATCC® CCL-247™) were purchased from ATCC (Manassas, VA, USA). Lastly, 008-FluoroSurfactant dissolved as 2% (w/w) in HFE-7500 was bought from RAN biotechnologies (Beverly, MA, USA) and HFE-7500 was acquired from 3M (Machelen, Belgium).

2.2. Cell culture, lentiviral transduction and preparation for microfluidics

To label different compartments of the cells, we generated the pLV-EF1α-3xFLAG NLS-mCherry-T2A-msfGFP-WPRE>PGK-Puro lentiviral vector by a Golden GateWay assembly protocol adapted for mammalian expression(31). HCT116 cells were transduced with concentrated lentivirus (in the presence of 8 μg/mL polybrene) at a multiplicity of infection of 1 and selected with puromycin at 2 μg/mL. The selected HCT116 cells stably express superfolder green fluorescent protein (msfGFP) in the entire cell (cytoplasm and nucleus) while mCherry is localized in the nucleus. Cells were maintained in McCoy's 5a Medium

supplemented with 10% FBS and 1% Penicillin/Streptomycin at 37°C in 5% CO_2. For microfluidic experiments, cells were dissociated using 0.05% Trypsin-EDTA, washed 2 times in DPBS and dissolved in DPBS supplemented with 2% FBS at a concentration of 2.5 x 10^6 cells/mL.

2.3. Microfluidic chip fabrication

The flow focusing and picoinjection designs are included in supplementary information (Fig. S1-3†). An SU8-mold was fabricated using standard soft-photolithography. For all molds, a 3-inch wafer was spin-coated with SU-8 2025 at 2000 rpm for 40 s to obtain a layer with height of approximately 40 µm. The wafer was baked at 65 °C for 3 min and at 95 °C for 6 min, followed by exposure at 160 mJ/cm². The wafer was then baked at 65 °C for 1 min and at 95 °C for 6 min, and subsequently developed for 5 min in PGMEA.

PDMS was mixed in a 10 to 1 ratio for the base elastomer and curing agent, degassed and poured over the wafer. After a bake at 80 °C for at least 2 h, the PDMS was cut and peeled off from the wafer. Inlet and outlet holes were punched with a 1 mm biopsy punch and the PDMS was cleaned with Scotch tape. The PDMS and glass surfaces were activated a plasma chamber (Blackhole Lab, Paris, France) for 2 min at high power, after which the PDMS was pressed onto the glass slide and baked overnight at 80 °C. The microfluidic channels were flushed with a solution of 1% trichloro(1H,1H,2H,2H-perfluorooctyl)silane in HFE-7500, after which the chip was placed in the oven for 2 h at 80 °C.

2.4. Microfluidic chip operation

Pressure pumps and flow sensors from the Fluigent (Le Kremlin-Bicêtre, France) LineUp series were used to control all liquid flows in the chip. Flow sensors were calibrated for the used liquids by connecting them to a syringe pump (PHD 22/2000, Harvard Apparatus, Cambridge, MA, USA), applying a range of flow rates, measuring the response of the flow sensors and inserting the calibration curve in the A-i-O software from Fluigent. Droplets of about 110 pL were generated using the flow focusing design. PBS was used as dispersed phase at 10 µL/min, while HFE-7500 with 2% of the fluorosurfactant, also referred to as 'oil', was used as continuous phase at 18 µL/min, both operated using a flow sensor (size Medium). Droplets were captured in a reinjection tube, which consisted of a 0.5 mL Eppendorf tube (VWR, Leuven, Belgium) with a punched hole of 1 mm at the top and the side of the tube. Microfluidic tubing was inserted and glued into each hole. The reinjection tube was filled with oil, the tubing attached to the side of the tube was connected through a flow sensor (size Small) with a pressure pump set at 0 mbar, and the tubing attached to the top of the tube was connected to the chip.

During picoinjection, the droplets from the reinjection tube were reinjected into the picoinjection chip at a flow rate of 2 µL/min. The oil was operated at 10 µL/min using a flow sensor size Medium. Picoinjectors were filled with PBS or with fluorescent dyes dissolved in PBS (400 µM for Alexa Fluor 350, 20 µM for fluorescein or 20 µM for Alexa Fluor 568) and operated using flow sensors size Small.

To determine cell lysis in droplets, flow focusing and serial picoinjection with 2 injectors were integrated into one microfluidic chip. The water phase, being DPBS supplemented with 2% FBS, was controlled at 2 µL/min using a flow sensor size Small, and the oil was operated at 10 µL/min using a flow sensor size Medium. To apply cells to the microfluidic chip, cells were loaded in a custom-made cell loading reservoir (Fig. S4). The first picoinjector was filled with DPBS, 400 µM Alexa Fluor 350 and 2% CHAPS, and the second picoinjector was filled with DPBS.

Electrode channels in the picoinjection chip were filled with a 5 M NaCl salt solution using a syringe with needle inserted in microfluidic tubing(32). A square wave of 20 kHz was generated by a pulse generator (TGP110, AIM-TTi, Cambridgeshire, United Kingdom), amplified (A600, FLC Electronics, Partille, Sweden) to 100 V and connected to the needle of the syringes using alligator clips. In a system with multiple injectors, each injector had a separate electrode and therefore a separate connection with the amplifier. The voltage was either passed onto the electrode or blocked by an Arduino-controlled 4-channel solid state relay (Seeed Studio 103020133 SPDT Relay, RS components, Brussels, Belgium).

2.5. Control algorithms, data acquisition and data analysis

Pressures and flow rates were measured using the A-i-O software from Fluigent. To control the pressure pumps as well as the electrodes in a multi-injector system, custom control software using MATLAB App Designer (Mathworks, Natick, MA, USA) was developed starting from the Fluigent software development kit(33). The built-in functions from the software development kit allowed to obtain flow rate and pressure measurements every 10 ms, and to control the pressure and flow rate of each liquid. Using these functions, a custom MATLAB script was built to calibrate and set the equilibrium pressure, apply linear curves to the injector flow rates, and (de)activate the electrodes.

For the calibration of the equilibrium pressure of an injector, different flow rates and pressures were first set for the oil, droplets and/or other injectors as shown in Tables S1-4†. Then, the pressure of the injector was manually varied until the equilibrium pressure of the injector was reached based on visual inspection. Afterwards, the corresponding pressures were recorded and saved by pressing a button in the software. After gathering all data, linear regression was performed on the data points and the obtained equation was later used in the software to turn off injection. During the time an injector was turned off, the equilibrium pressure was updated in real-time based on measurements of the oil pressure, at a sample rate of 10 ms. Using MATLAB, analysis of covariance(34,35) was performed on the obtained linear equations to compare slope and intercept of different models ($\alpha = 0.05$).

To perform time-invariant picoinjection, injector flow rates were set for prolonged times (e.g. 10 min) using the built-in functions from the software development kit. To enable

sweeping of the injector flow rates during time-variant picoinjection, a linearly varying input was given to the function of the software development kit that allowed to control the injector flow rate. The input was increased or decreased every second, with step sizes depending on the sweep time and final or initial flow rate. For example, to sweep flow rates from equilibrium pressure until 2.5 µL/min within 1 min as in section 3.4.1, the input was first set to equilibrium pressure. Then, upon starting the sweep, the applied flow rate started at 0.1 µL/min and increased every second with steps of 0.04 µL/min until the final flow rate of 2.5 µL/min was reached.

Upon turning an injector on or off, by setting a flow rate or the equilibrium pressure, electrodes were activated or deactivated, respectively, by sending an input to the Arduino that was coupled to the 4-channel solid state relay as described above. The maximal operation time of the relay was 10 ms, and a commercially available Arduino library was used to control the relay(36).

To determine the stabilization time after changing a picoinjector setting, all possible setting alterations (Table S5†) were tested and measured in triplicate. The stabilization time was defined as the time between (i) the moment at which the injector pressure and flow rate values deviated more than 1 mbar and 0.05 µL/min respectively when compared to the initial values, and (ii) the moment at which the injector pressure and flow rate values did not deviate more than 1 mbar and 0.05 µL/min respectively when compared to the final values.

The microfluidic chip was positioned on the stage of an inverted Olympux IX-73 microscope (Tokyo, Japan) equipped with a high speed camera (Phantom Micro C110, Vision Research, Wayne, NJ, USA) and 2 photomultiplier tubes (PMTs) (PMM02, Thorlabs, NJ, USA) for the detection of GFP and mCherry (Fig. S5†). Droplet frequency was determined by analyzing the peaks of the PMT signal for fluorescent droplets in MATLAB. To image droplets in wide-field, droplets were pipetted into KOVA glasstic slides. Droplet diameters were determined based on bright field images using a MATLAB script for the detection of circles. The coefficient of variation (CV) of droplet sizes was calculated by dividing the standard deviation in droplet diameter by the average droplet diameter and multiplying by 100. Since the height of the KOVA slides (100 µm) was higher than the droplet diameter, droplets were assumed to be spherical for droplet volume calculations.

Fluorescent wide-field imaging of droplets was performed on an inverted microscope (Nikon Ti-Eclipse Tokyo, Japan) at 15x magnification using DAPI, FITC and TRITC filters. For each wavelength, multiplicative shading correction was performed inside the NIS elements software (Nikon, Tokyo, Japan) using fluorescent dye squeezed between glass slides as correction image. Overlays of fluorescent images were made in ImageJ after setting all images of a certain wavelength to the same display range, and assigning a gray, blue, green, or red color to the bright field, DAPI, FITC or TRITC images, respectively. The intensity at each fluorescent wavelength was determined using ImageJ 1.52p (National Institutes of Health, USA) by first detecting the droplet outlines on a bright field image, and afterwards determining the mean intensity of these regions for each wavelength.

For the detergent concentration screening for cell lysis in droplets, time-invariant picoinjection was performed to construct a calibration curve between the CHAPS concentration and the intensity of a blue fluorescent dye that was loaded together with the CHAPS solution, whereas time-variant picoinjection with 2 opposite linear curves was performed to screen a dense CHAPS concentration range. First, droplets formed by time-invariant picoinjection at different flow rates were captured and imaged. By analyzing droplet volume before and after picoinjection, the volume added by the injector with the 2% CHAPS solution and thus the CHAPS concentration in the droplet was calculated. This concentration was correlated with the intensity of the blue fluorescent dye. The resulting calibration curve was used to determine the CHAPS concentration in droplets obtained in the time-variant picoinjection experiment. Moreover, the calibration curve was used to determine the achieved CHAPS concentration range by time-variant picoinjection, for which the highest blue fluorescent intensity was defined by the highest measured intensity, and the lowest blue fluorescent intensity was defined as the average background intensity plus three times the standard deviation of the background intensity. For this, the blue fluorescent background intensity was determined by the fluorescent intensity of the droplets into which no CHAPS solution or blue dye was injected during the time-invariant picoinjection experiment. Cell lysis of the membrane and nucleus was monitored by the release of GFP and mCherry out of the cell into the droplet using FITC and TRITC images, respectively. Based on manual inspection in ImageJ, lysis was defined as the condition in which the droplet showed higher fluorescence than the background, and no fluorescent cell could be observed within the droplet. Only droplets containing fluorescent single cells were taken into account. For each cell, the presence (1) or absence (0) of membrane and nuclear lysis was noted. For both membranal and nuclear lysis, multiple logistic regression models(37,38) were constructed to analyze the influence of detergent concentration and incubation time on the probability of lysis using JMP Pro 15 (SAS, Cary, NC, USA). In JMP, inverse prediction was performed to estimate the detergent concentration to achieve 99% cell lysis, resulting in a predicted concentration and an asymmetric 95% confidence interval (CI).

3. Results and discussion

3.1. Concept of picoinjection using combined pressure and flow rate control

To be able to control both the pressure and flow rate of the injector liquid, pressure pumps were used in combination with flow sensors. In this set-up (Fig. 1a), each reagent reservoir was pressurized through an air tube, causing liquid to flow into the fluidic tubes, through a flow sensor, towards the microfluidic chip. Custom control software, based on a software development kit(33,39), was used to control either the applied

pressure or flow rate of each picoinjector. When a certain flow rate was set, the control software adapted the applied pressure to reach the required flow rate. First, droplets of about 110 pL were generated by flow focusing and stored in a reservoir, after which they were reinjected into the picoinjection chip where they were spaced by oil (Fig. 1b). Here, the flow rate of the droplets and the oil was controlled at 2 and 10 µL/min respectively, reaching a droplet frequency of about 350 droplets per second.

To perform reagent addition into droplets, the flow rate of the picoinjector was controlled while the electrodes were actuated. When a certain flow rate was set, the liquid in the picoinjector bulged out into the main channel, and merged with passing droplets because of the electric field (Movie S1†). Once the flow rate exceeded a certain value, in this case above 2.5 µL/min, the injector formed droplets into the main channel at a higher rate than the frequency of the passing droplets, resulting in faulty injection (Movie S2†). Therefore, during injection, the flow rate of the injector was controlled until a maximum of 2.5 µL/min.

To turn off reagent addition by a picoinjector, the electrodes were deactivated and the pressure of the injector was set at its equilibrium pressure, which resulted in a stable interface between the injector liquid and the main channel (Movie S3†). To automatically set the correct equilibrium pressure, linear models were constructed between the equilibrium pressure of each injector and the pressure of the oil. Upon setting the equilibrium pressure, the pressure of the injector was adapted

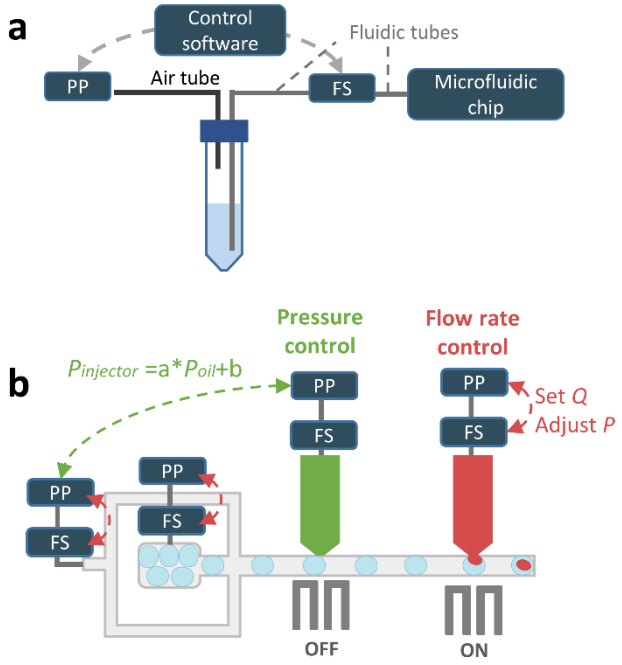

Figure 1: Set-up for picoinjection experiments. (a) Schematic representation of the pressure pumps and flow sensors. (b) Set-up for combined pressure and flow rate control for picoinjection. When picoinjection was turned off, electrodes were deactivated and pressure control was used, for which a linear model was determined between the equilibrium pressure of the injector and the pressure of the oil. When picoinjection was turned on, electrodes were activated and flow rate control was used. PP = Pressure Pump, FS = Flow Sensor, Q = flow rate, P = pressure.

in real-time by the control software using the calibrated relationship with the oil pressure.

3.2. Calibration of the picoinjector equilibrium pressure

3.2.1. One single picoinjector. First, the optimal equilibrium pressure of an injector was determined. Three different equilibrium pressures were defined based on visual inspection: (i) the minimal equilibrium pressure (P_{min}), which was the lowest pressure at which the injector liquid did not retract back into the picoinjector channel, (ii) the maximal equilibrium pressure (P_{max}), which was the highest pressure at which the liquid did not bulge out of the injector, and (iii) the mid-equilibrium pressure (P_{mid}), which was the pressure at which the water-oil interface was located in the middle of the narrow injector orifice (Fig. 2a). To obtain linear models for these pressures within one microfluidic chip, several combinations of oil and droplet flow rates were set (Table S1†), after which the pressure of the injector was varied manually to reach the equilibrium pressure, followed by recording of the pressure data. It was observed that all of the defined equilibrium pressures were linearly correlated ($R^2 > 0.9635$) with the pressure of the oil, with P_{mid} being positioned in between P_{min} and P_{max} (Fig. 2a). The linear model for P_{mid} was used to turn off picoinjection in all following experiments, since slight over- or underestimation of P_{mid} was tolerated because of the boundaries set by P_{min} and P_{max}.

Additional tests showed that the linear model depended on the droplet size (Fig. S6a†) and that it was different for each microfluidic chip given a fixed droplet size (Fig. S6b†), but that it was stable over time in the same chip for a fixed droplet size (Fig. S6c†). Moreover, the equilibrium pressure was higher for injector liquids with higher viscosity due to the presence of 10% or 20% glycerol (Fig. S6d†). A pressure calibration before the start of each experiment thus allowed (i) to control for chip-to-chip variation as a result from manual chip fabrication, (ii) to correct for differences in droplet size between experiments, and (iii) to switch between different injector liquids as required by the application.

3.2.2. Two serial picoinjectors. The ability to turn off an injector by pressure control is especially useful for a system with 2 or more injectors in series, since it enables to inject one reagent but not the other(s). In a 2-injector system, it was observed that for a fixed flow rate for the oil and the droplets, the pressures required to reach those flow rates were influenced by the flow rate applied to each injector (Fig. S7†). This indicated that the pressure in the main channel was affected by the setting of one injector, which consequently had an impact on the equilibrium pressure of the other injector. Therefore, the equilibrium pressure of each picoinjector was calibrated using a fixed oil and droplet flow rate, while varying the applied flow rate of the other injector between 0.5 and 2.5 µL/min in steps of 0.5 µL/min, or setting the equilibrium pressure of the other injector (Table S2†). It was observed that the equilibrium pressure of each injector was linearly correlated ($R^2 > 0.9794$) with the pressure measured for the oil, and that the lowest and highest obtained values for the equilibrium pressures differed up to 60

mbar per injector (Fig. 2b). Additionally, the equilibrium pressures of the injector closest to the outlet were lower than those of the other injector, which can be explained by the pressure drop typically present in microfluidic channels.

These results demonstrate the importance of controlling the pressure of a deactivated injector based on a calibrated relationship with the oil pressure. Multi-injector systems that solely rely on pressure control without any feedback system are limited in the possible range of injected volumes since large changes in pressure of one injector will destabilize the other(s). Although this might be solved by visual inspection of the injector liquid interface and manually adjusting the pressure of the other injector, such an approach would be cumbersome, less robust and not user-friendly.

3.2.3. Three serial picoinjectors. Similar as for 2 picoinjectors, the equilibrium pressure of each picoinjector in a 3-injector system was calibrated by using a fixed flow rate for the oil and the droplets, while the other picoinjectors were either set at equilibrium pressure or at a flow rate ranging from 0.5 to 2.5 µL/min. To cover every possible combination of equilibrium pressures and flow rates, 36 measurement points were required to fully calibrate each injector (Table S3†). It was again observed that the equilibrium pressure of each injector was linearly correlated ($R^2 > 0.9484$) with the pressure of the oil, and that it was lower when the injector was positioned more closely towards the outlet (Fig. 2c). Here, the lowest and highest obtained value for the equilibrium pressures differed up to 137 mbar per injector. Additionally, it was important that the channel after the last picoinjector was sufficiently long to ensure the equilibrium pressure of the last injector was above 50 mbar, as lower pressures resulted in less accurate model estimations and thus less robust control of the equilibrium pressure (Fig. S8†).

Since it is too cumbersome to calibrate a 3-injector system before each experiment with 36 measuring points per injector, a less extensive calibration set was constructed with only 7 measurement points, in which each injector was either set at equilibrium pressure or at the maximal flow rate of 2.5 µL/min (Table S4†). With these 7 points, 4 equilibrium pressure values for each injector were obtained, allowing determination of the linear models with similar accuracy ($R^2 > 0.9712$) as compared to those obtained with the full calibration procedure (Fig. 2d). Additionally, the intercepts and slopes of the models estimated by the short calibration procedure showed no significant difference from those estimated by the full calibration procedure as determined by analysis of covariance(34). As such, precise calibration of the equilibrium pressures of the 3-injector system was obtained within only 10 min.

To summarize, a quick calibration of the equilibrium pressures of serial picoinjectors before each experiment allows to compensate for (i) droplet sizes, (ii) chip-to-chip variation, (iii) differences in injector liquid viscosity, and (iv) pressure fluctuations in the main channel induced by settings of other picoinjectors. We expect that this approach is expandable to systems with even more injectors, as well as to systems with different configurations, e.g., when 2 injectors are positioned

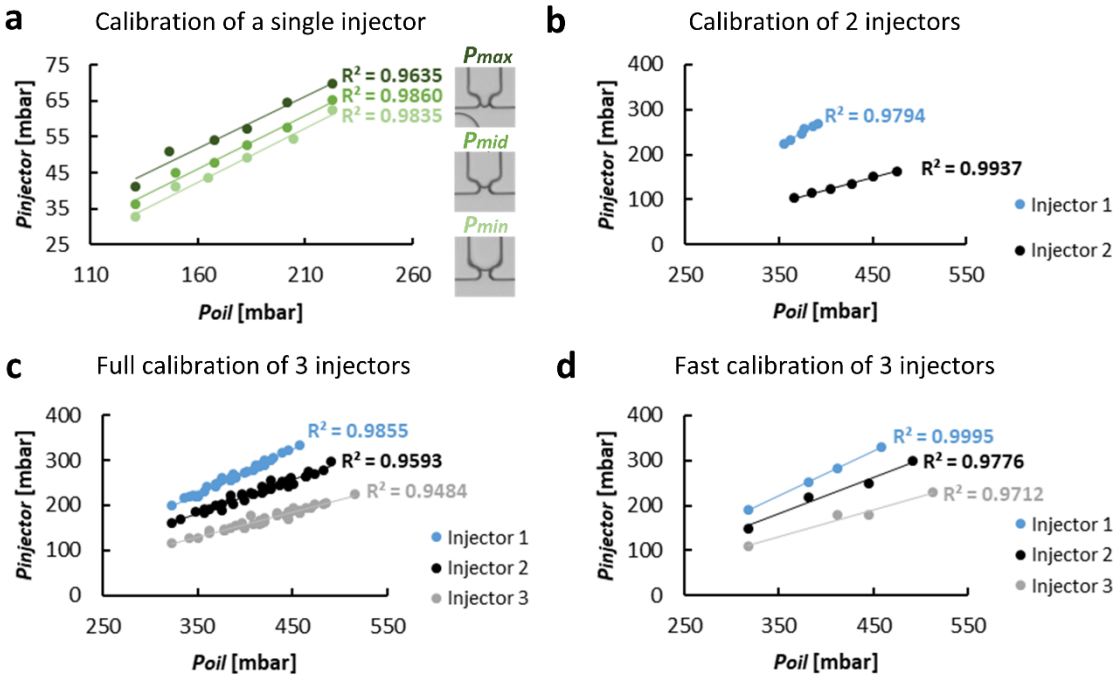

Figure 2: Calibration of the equilibrium pressure of 1, 2 and 3 injectors. (a) Calibration of a single injector. Three equilibrium pressures were defined: P_{max}, P_{mid} and P_{min}. All equilibrium pressures were linearly correlated with the pressure of the oil. (b) Calibration of 2 serial injectors. Linear relationships were found between the equilibrium pressure (P_{mid}) of both injectors and the oil pressure. (c) Full calibration of 3 serial injectors, which requires many measurement points. Linear relationships were found between the equilibrium pressure (P_{mid}) of all injectors and the oil pressure. (d) Fast calibration of 3 serial injectors with only 7 measurement points. Linear models with similar accuracy were obtained as compared to the models found by the full calibration procedure. The intercepts and slopes of the models estimated by the fast calibration procedure showed no significant difference from those estimated by the full calibration procedure as determined by analysis of covariance. *P* = pressure.

before and after an incubation channel. We furthermore obtained data supporting that similar pressure relationships were found in microfluidic designs with smaller dimensions using 4 pL droplets (Fig. S9†). As future work, it can be of interest to automate the calibration procedure by sweeping different flow rate and pressure settings of the injectors and/or the droplets and oil, while monitoring the picoinjector liquid interface to determine when the equilibrium pressure is reached using image analysis.

After calibration, the obtained linear model for each picoinjector was incorporated into the custom control software. The model was then applied when an injector was turned off, and the software allowed to update the equilibrium pressure in real-time based on measurements of the oil pressure at a sample rate of 10 ms. In the following, we illustrate the use of flow rate control to vary the injected volume by a picoinjector, as well as the use of these linear models to stop picoinjection.

3.3. Picoinjection with time-invariant settings

3.3.1. One single picoinjector. As a first concept, picoinjection with time-invariant settings was performed, in which the injector was set at a certain value for 10 min and the droplets obtained by each setting were collected in a separate reservoir (Fig. 3a). To perform reagent addition into droplets, the flow rate of the picoinjector was controlled between 0.5 and 2.5 µL/min, in steps of 0.5 µL/min, while the electrodes were actuated. When no injection was performed, the equilibrium pressure was set based on the linear model determined as above, and the electrodes were deactivated.

Upon changing the setting of the picoinjector, the pressure of the injector was adapted by the control software to achieve the desired flow rate or the equilibrium pressure (Fig. S10†). Since the pressure applied to the injector liquid had an influence on the pressure in the main channel of the microfluidic chip, the pressure of the droplets and the oil had to be adapted as well to again attain the required flow rates. This resulted in a stabilization time of 8.2 ± 3.3 s to switch between injector flow rates (Fig. S10a-c†), 14.0 ± 2.9 s to adapt from equilibrium pressure to a certain flow rate (Fig. S10d-f†), and 4.3 ± 1.9 s to turn off an injector by setting the equilibrium pressure (Fig. S10g-i†). During the stabilization periods, the resulting droplets were discarded.

Based on the applied injector flow rates and the observed droplet frequency of 357 droplets per second, the expected injected volume was calculated for each condition. It was observed that droplet volume increased linearly with the injector flow rate (Fig. 3b), showing high correspondence with the estimated droplet volume (Fig. 3c). Moreover, droplets remained highly monodisperse after injection (CV droplet diameter <2%) (Fig. 3d), indicating robust reagent addition. Lastly, although droplet volume could be doubled in this picoinjector system, the distributions become broader at higher injector flow rate (Fig. 3e), indicating more variation of the injected volume at those settings, which has to be taken into

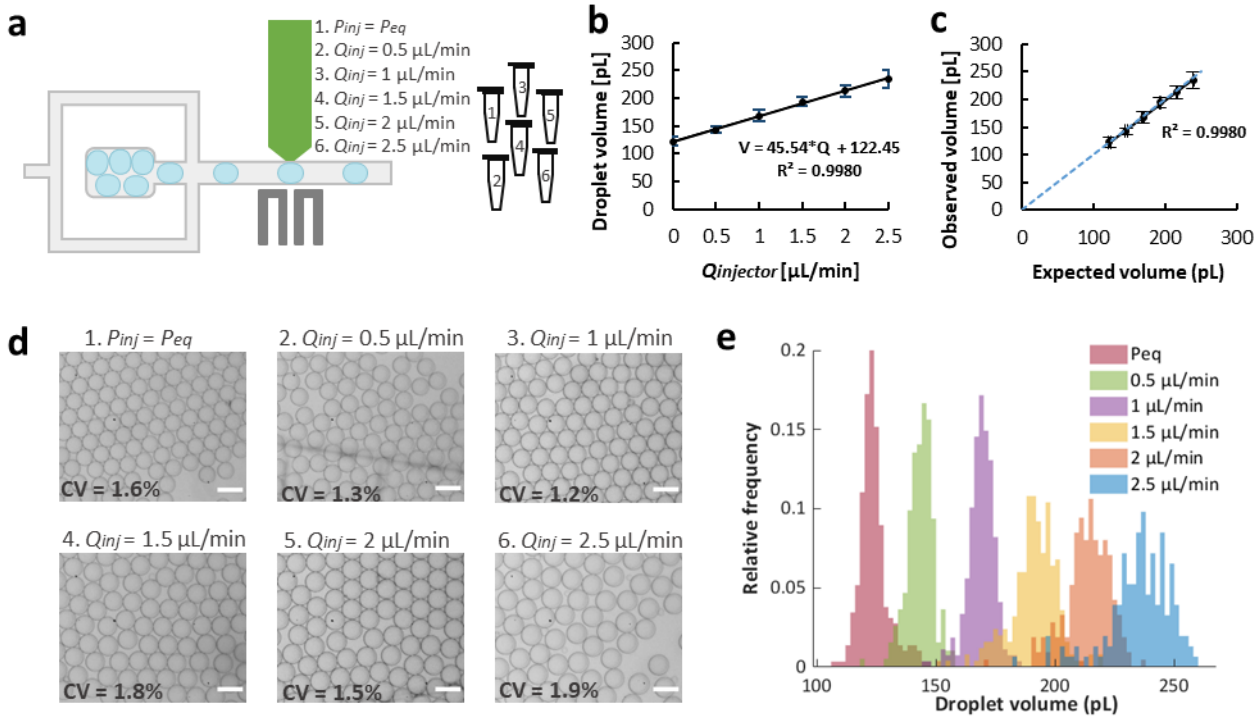

Figure 3: Picoinjection with time-invariant settings using 1 single injector. (a) The picoinjector was either set at its equilibrium pressure, or at a certain fixed flow rate. For each picoinjector setting, the resulting droplets were collected in a separate reservoir. (b) Droplet volume increased linearly with the flow rate of the injector. In practice, the value for the condition Q_{inj} = 0 µL/min was obtained by setting the equilibrium pressure. At least 153 droplets were measured per setting. (c) The observed droplet volume corresponded to the expected droplet volume as calculated based on the injector flow rate, the droplet frequency and the initial droplet size. Dots represent the average droplet volume obtained for each injector setting, and error bars represent one standard deviation to the mean. (d) Bright field microscopy images of highly monodisperse droplets obtained by different picoinjector settings. Scale bar = 100 µm. (e) Relative frequency distributions of droplet volumes for each injector setting. *P* = pressure, *Q* = flow rate, *inj* = injector, *eq* = equilibrium, *V* = volume.

account when implementing picoinjection for a certain application. Occasionally, unexpectedly small or large droplets were observed, which could be explained by sporadic, spontaneous coalescence of droplets during the reinjection process.

Although pressure control might also be used to perform reagent addition(17), the pressure to obtain a certain flow rate would depend on the other pressures in the microfluidic chip and on the viscosity of the injector liquid. Here, for example, picoinjection of more viscous liquid containing 20% glycerol could be achieved by flow rate control using calibrated flow sensors (Fig. S11a†). Therefore, flow rate control is preferred to inject predefined volumes into droplets, which is essential in experiments that require a specific concentration of the supplemented compound. Lastly, we showed that the picoinjection method could also be applied for injection into smaller droplets of about 5 pL (Fig. S11b†).

3.3.2. Three serial picoinjectors. Next, picoinjection with time-invariant settings was applied to a system with 3 serial injectors (Fig. 4a). Each injector was loaded with a blue, green or red fluorescent dye, and the settings of the injectors were carefully selected to result in droplets with the same final volume. More specifically, each injector was controlled independently at either equilibrium pressure or a flow rate of 0.5, 1, 1.5 or 2 µL/min, and the sum of the applied flow rates was chosen to be 2 µL/min, resulting in 15 different injector conditions (Table S6†).

As a result, a library of droplets with different fluorescent dye concentrations was created (Fig. 4b). For each condition, droplets were highly monodisperse (CV droplet diameter <3.4%) and the average droplet volume ranged between 183 and 194 pL. The droplet volume distributions were wider after injection when compared to before injection, indicating a slight variation on the injected volume (Fig. 4c). Nevertheless, the average fluorescent intensity of each dye was highly correlated with the injector flow rate, and the variance in intensity of each dye between the droplets was low (CV < 8.5%), pointing to accurate reagent addition for each injector setting (Fig. 4d). Moreover, for conditions in which one or more of the injectors were turned off, the corresponding fluorescent dyes were not observed in any of the resulting droplets, indicating precise control of the equilibrium pressure based on the linear models.

The illustrated picoinjection approach is for example of interest in drug interaction studies, for which the final drug concentration has to be precisely controlled. Here, 2 injectors could contain 2 types of drugs with expected interactions, while the third injector could inject buffer for volume compensation. Although we demonstrated a case with fixed droplet volume, other combinations of flow rates can be selected as well to vary the final droplet volumes. Separate collection of droplets for each injection condition is especially useful for experiments in

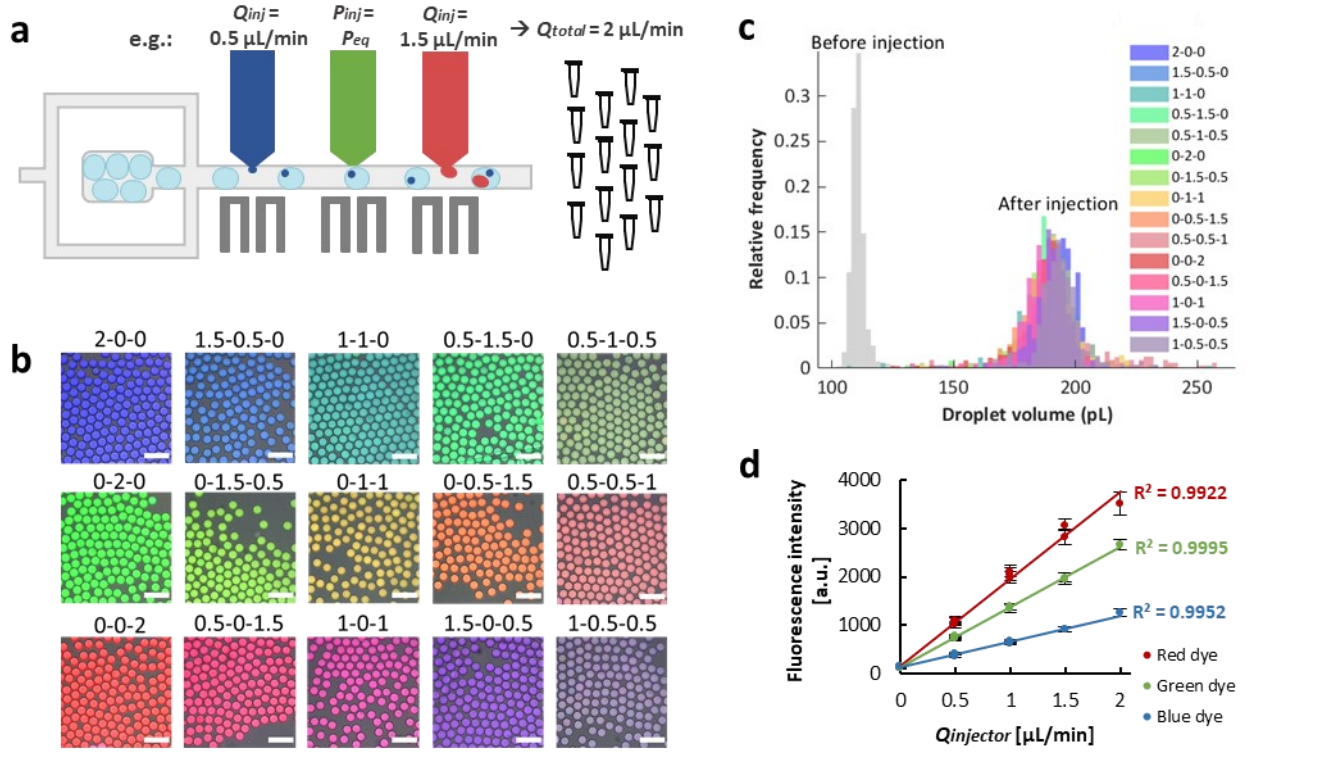

Figure 4: Picoinjection with time-invariant settings using 3 serial injectors, containing a blue (Alexa Fluor 350), green (fluorescein) or red (Alexa Fluor 568) fluorescent dye. (a) Each picoinjector was either set at its equilibrium pressure, or at a certain fixed flow rate, while the sum of all flow rates was always 2 µL/min. For each setting, the resulting droplets were collected in a separate reservoir. (b) Fluorescent overlay images of highly monodisperse droplets with different colours obtained by different picoinjector settings. Above each image, the picoinjector settings are noted with units in µL/min, in which 0 corresponds to setting the equilibrium pressure. The first, second and third number correspond to the injector containing the blue, green and red dye, respectively. Scale bar = 200 µm. (c) Relative frequency distributions of droplet volumes for each injector setting. The injector conditions in the legend were noted as in b. (d) The average fluorescent intensity of droplets injected with a certain dye was linearly correlated with the flow rate of the injector containing that dye. At least 350 droplets were measured per condition. Dots represent the average fluorescent intensity and error bars represent one standard deviation to the mean. The intercept represents background noise. *P* = pressure, *Q* = flow rate, *inj* = injector, *eq* = equilibrium.

which the injected reagent diffuses between droplets of different concentrations, or when fluorescent dyes cannot be used as a marker to indicate the injected volume per droplet.

3.4. Picoinjection with time-variant settings

3.4.1. One single picoinjector. Besides time-invariant picoinjection, picoinjection with time-variant settings was also demonstrated, in which the setting of the injector was continuously varied by sweeping different injector flow rates, and all resulting droplets were collected in one reservoir (Fig. 5a). Here, the setting of the injector was programmed to vary linearly from zero flow rate (equilibrium pressure) to the maximal flow rate of 2.5 µL/min within 1 min. As a result, the measured flow rate of the injector liquid increased gradually (Fig. 5b). Upon injecting a green fluorescent dye, the fluorescent intensity, measured with a PMT positioned at the end of the microfluidic channel, gradually increased according to the applied injector flow rate (Fig. 5b). Based on the measured flow rates and PMT signals, it was observed that the linear increase from minimal to maximal flow rate could be performed within 30 s, but that the pressure pumps were lagging behind when faster inputs were applied (Fig. S12†). Picoinjection with time-variant settings resulted in a droplet library of different sizes (Fig. 5c), for which droplet size was correlated with fluorescent intensity (Fig. 5d).

Since all droplets are pooled in this method, it is required to measure either droplet size or intensity of a fluorescent additive to link the injected volume per droplet to the observed effect in that particular droplet. The use of a fluorescent additive in the injector is especially useful when analyzing the droplets with laser-induced fluorescence, using for example a PMT, since this method does not allow to distinguish droplet sizes.

3.4.2. Two serial picoinjectors. Picoinjection with time-variant settings was also applied for 2 injectors in series, for which the second injector was used to compensate for the liquid injected by the first injector, to obtain droplets with the same final volume (Fig. 6a). Each injector was loaded with a green or red fluorescent dye, and opposite flow rates were applied. After injection, 2 PMTs were used to measure the fluorescent intensity of the droplets for both dyes, and their signals increased or decreased as expected based on the applied injector flow rates (Fig. 6b). As a result, a library was created with highly monodisperse droplets (CV droplet diameter <2.4%) (Fig. 6c), and the fluorescent intensities of the 2 dyes were negatively correlated (Fig. 6d).

In a system with multiple injectors with time-variant settings, droplet size measurements are no longer suited to determine the volume added by each injector. Therefore, it is essential that fluorescent markers are used as an additive to derive the injected volume per picoinjector, for both laser-induced fluorescence measurements and wide-field imaging. In case the final volume of the droplets is fixed as in our proof-of-concept, a fluorescent additive for only one of the injectors suffices. Although we only illustrated linearly varying injector flow rates and fixed end-volumes, other signal shapes can be

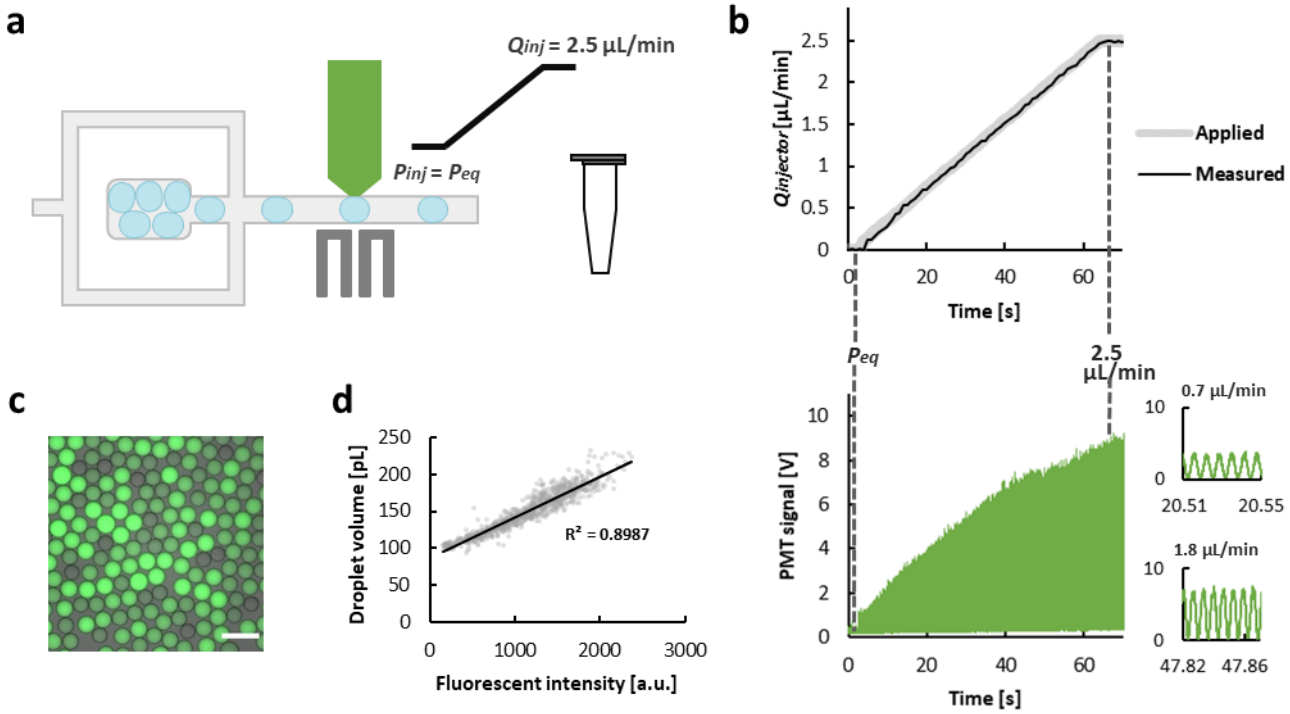

Figure 5: Picoinjection with time-variant settings using 1 single injector containing green fluorescent dye (fluorescein). (a) The picoinjector setting was varied from zero flow rate (equilibrium pressure) to a flow rate of 2.5 µL/min in the course of 1 min. All droplets were collected in the same reservoir. (b) The measured injector flow rate corresponded to the applied flow rate. Simultaneously, the signal of the PMT measuring the fluorescent droplet intensity increased from baseline to maximal value. Zoom-ins of the PMT signal are shown for 3 different flow rates to illustrate the individual droplet peaks with different heights obtained for those injector settings. (c) Fluorescent overlay image of droplets with various sizes and intensities. Scale bar = 100 µm. (d) Droplet volume and fluorescent intensity were linearly correlated, indicating that both parameters can be used to determine the injected volume per droplet. 955 droplets were analysed. *P* = pressure, *Q* = flow rate, *inj* = injector, *eq* = equilibrium.

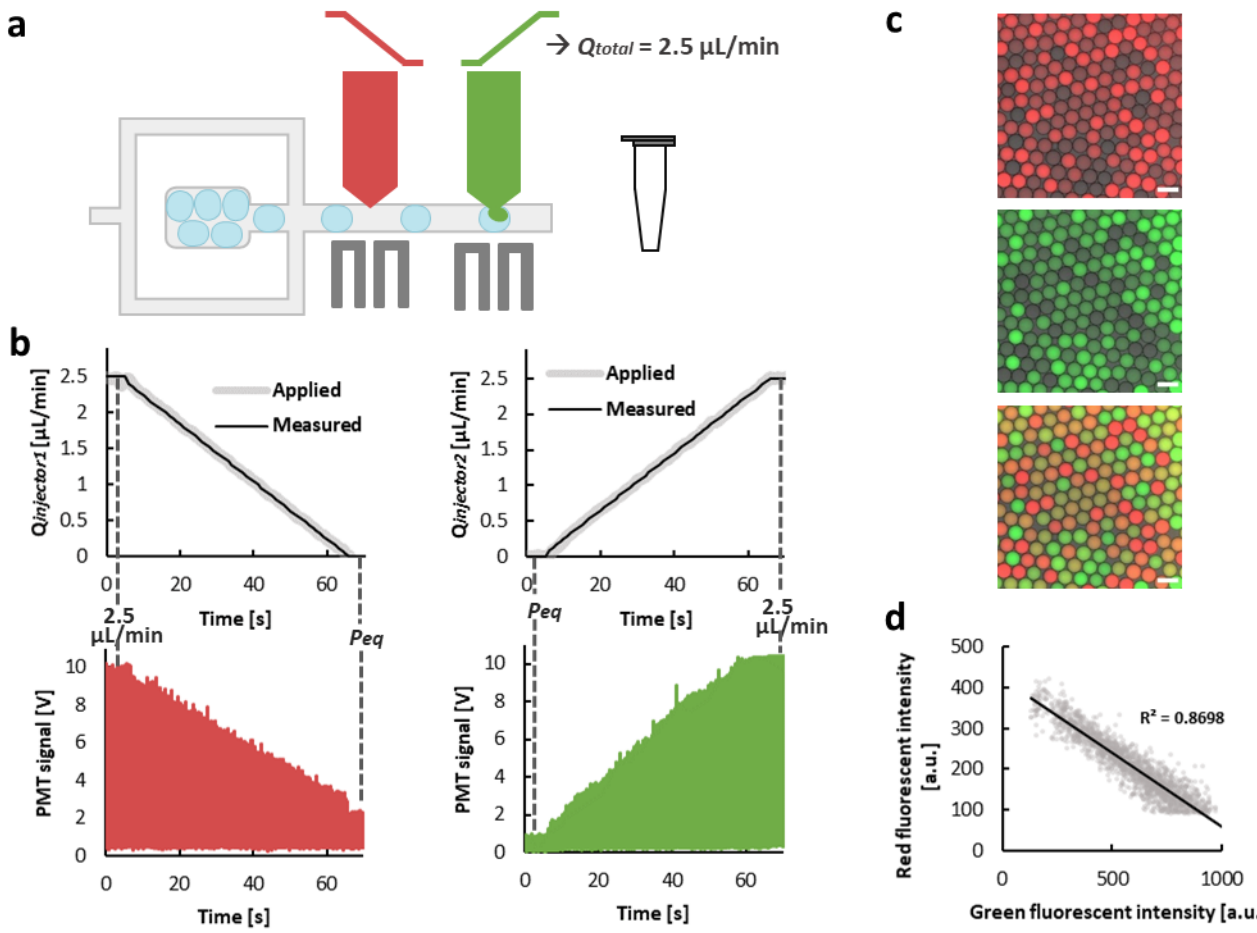

Figure 6: Picoinjection with time-variant settings using 2 serial injectors containing a green (fluorescein) or red (Alexa Fluor 568) fluorescent dye. (a) Picoinjector settings were continuously varied using opposite linear curves, to result in droplets with a fixed final volume. All droplets were collected in the same reservoir. (b) The measured injector flow rate corresponded to the applied flow rate for both injectors. Simultaneously, the signal of the PMTs measuring the fluorescent droplet intensity increased from maximal value to baseline or vice versa. (c) Fluorescent overlay image of droplets with uniform sizes and varying intensities. Scale bar = 100 µm. (d) Red and green fluorescent intensities were negatively correlated. 1839 droplets were analysed. *P* = pressure, *Q* = flow rate, *eq* = equilibrium.

applied to the injectors as well to achieve different final volumes, if required by the application.

When the research equipment and application allow to use fluorescent additives, picoinjection with time-variant settings is an attractive method since the entire picoinjection process is performed automatically, resulting in a pooled droplet library with a high variation of reagent concentrations, thereby allowing for fast screening of all obtained droplets. For example, the 2-injector system described in this work could be used for fast compound concentration screenings, to determine e.g., the minimal inhibitory concentration of an antibiotic(40,41) or antimycotic, the required detergent concentration to achieve cell lysis in droplets, or the reaction rate of an enzyme in combination with a certain substrate(42). Different amounts of the reagent can be added to the droplets using the first injector, while the second injector ensures a fixed end-volume of the droplets. By supplementing the first injector with a fluorescent dye, the concentration of the compound per droplet can be measured, while another fluorescence wavelength or bright field measurements can be used to analyze the response inside the droplets. Meanwhile, picoinjection with time-invariant settings remains of interest for applications in which injected reagents may diffuse between droplets of varying concentrations, or when it is not possible to use fluorescent additives, e.g., when the equipment cannot measure fluorescence or when it can only measure fluorescence at a few wavelengths but those wavelengths are required to study the response in the droplets. Summarized, our novel methodology allows to tailor the configuration and operational parameters of serial picoinjectors, allowing a wide implementation of the technology in numerous life science applications.

3.5. Detergent concentration screening for cell lysis in droplets

To illustrate the potential of the serial picoinjection technology for fast compound concentration screenings, the zwitterionic detergent CHAPS was injected into droplets containing single cells, followed by monitoring lysis of the cellular membrane and nucleus. To this end, the droplet generation chip was integrated with 2 serial picoinjectors, of which the first was loaded with DPBS containing 2% CHAPS and a blue fluorescent dye, and the second was loaded with DPBS (Fig. 7a). The sum of the applied flow rates of the injectors was kept constant to result in droplets with the same final volume. First, droplets without cells were generated, and time-invariant picoinjection was performed (Table S7†), allowing to correlate the blue fluorescence intensity of the droplets to the flow rate of the first injector. The

injected volume and consequently the concentration of CHAPS in the droplets was calculated based on the known injector flow rate, initial droplet volume and droplet frequency, allowing to construct a calibration curve between the fluorescence intensity and the CHAPS concentration (Fig. 7b). Next, single cells expressing GFP in the entire cell and mCherry in the nucleus were encapsulated in droplets and time-variant picoinjection was performed. Bright field and fluorescent images were taken at 0 h, 1 h and 2 h after droplet library generation. The CHAPS concentration was calculated based on the blue fluorescence intensity of the droplets, and lysis of the membrane and nucleus was determined by the release of GFP and mCherry into the droplet (Fig. 7c). More specifically, the absence or presence of lysis was labeled with a 0 or 1, respectively. Then, for both lysis of the membrane and the nucleus, multiple logistic regression models were constructed (Fig. 7d, Fig. S13† and Table S8†) that enabled to predict the fraction of lysed cells for a certain CHAPS concentration and incubation time. For example, to obtain membrane or nuclear lysis in 99% of all cells after 1 h, a CHAPS concentration of 0.70% (95% CI [0.64%, 0.77%]) or 0.92% (95% CI [0.86%, 1.01%]) is required, respectively (Fig. S14†). As such, within a single experiment, we screened a dense detergent concentration gradient (0.06% - 1.01%) and determined the minimally required concentration of the detergent to achieve lysis of the cellular membrane and nucleus. These type of data are valuable for studies on intracellular compounds, since lysis agents can influence other reactions in droplets and their concentration should therefore be minimized. Moreover, these type of picoinjection protocols are highly useful for the optimization of single-cell workflows in droplets.

With respect to concentration gradient formation in droplets, several other microfluidic techniques have been described. These methods for example rely on passive co-flow of reagents(42) or controlled coalescence(43) in smart channel geometries, on controlled dosing of reagents by syringe pumps

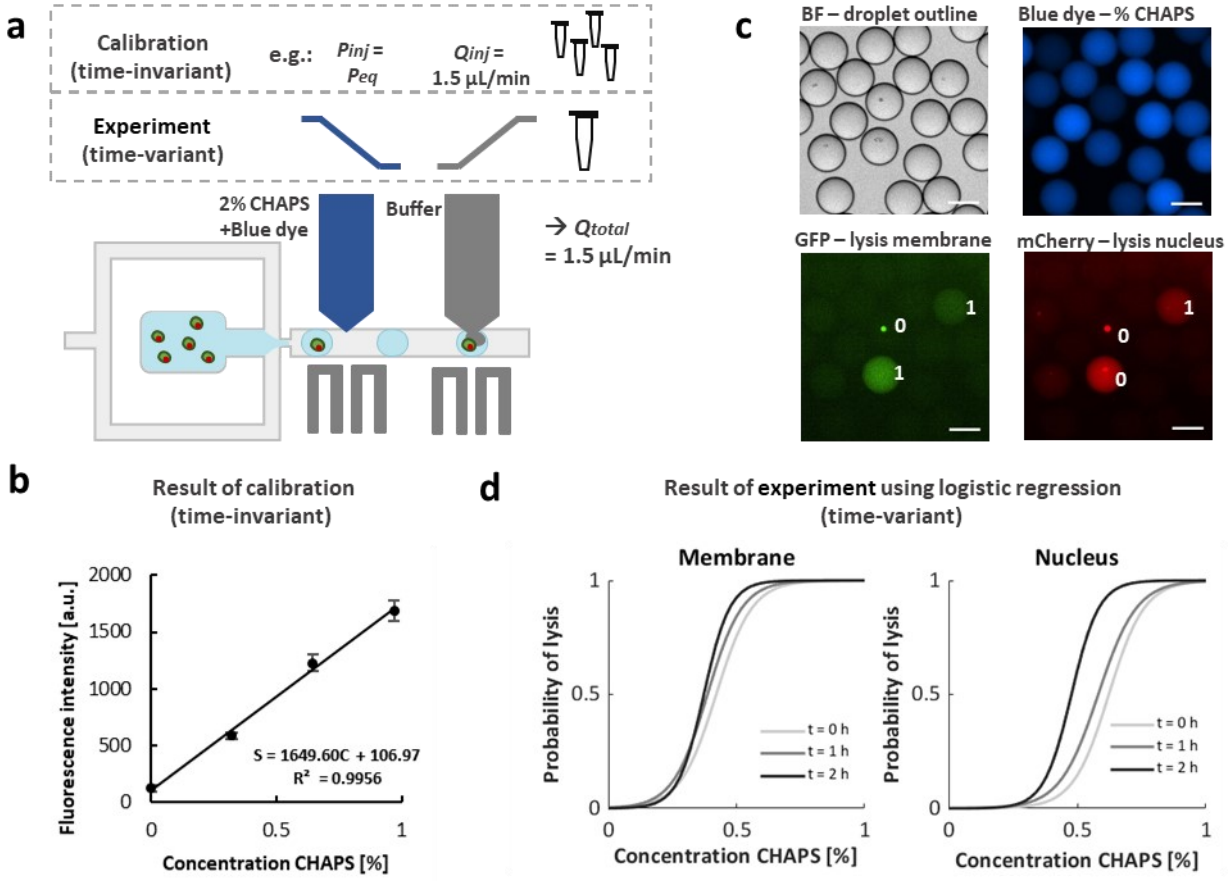

Figure 7: Detergent concentration screening for cell lysis in droplets using 2 serial picoinjectors. (a) Set-up of the experiment. Two serial injectors were integrated with droplet generation on a single chip. Time-invariant picoinjection at 4 different settings was used to correlate the fluorescent intensity of the droplets (originating from the blue dye Alexa Fluor 350) to the CHAPS concentration. Time-variant picoinjection was used to add varying amounts of CHAPS to droplets containing single cells. (b) Calibration curve between blue fluorescent intensity and concentration of CHAPS. For each condition, minimally 100 droplets were analysed. Dots represent the average fluorescent intensity, and error bars represent one standard deviation to the mean. (c) Example microscopy images with 3 droplets containing fluorescent single cells. Bright field images were used to determine droplet outline. DAPI images (blue) were used to determine the fluorescent intensity of the droplets and thereby calculate the concentration of CHAPS in the droplet. FITC images (green) were used to study the release of GFP out of the cytoplasm of the cell and thus monitor membrane lysis. TRITC images (red) were used to study the release of mCherry out of the nucleus of the cell and thus monitor nuclear lysis. Lysis was defined as the condition in which the droplet was fluorescent and no fluorescent cell could be observed. Only droplets with single, fluorescent cells were included in the analysis. As an example, 3 cells are marked with 0 or 1 to indicate absence or presence of lysis respectively. Scale bars indicate 50 µm. (d) Logistic regression models were constructed to examine the effect of time and CHAPS concentration on the probability of lysis of both the membrane and nucleus. Minimally 500 cells were analysed per time point. S = signal, C = concentration, *Q* = flow rate, *P* = pressure, *inj* = injector, BF = bright field, t = time.

prior to chip loading(41), on droplet-on-demand systems followed by electro-coalescence(40) or passive droplet fusion(44), or on plug generation by valve-based systems (45) or aspiration from 96-well plates(46) followed by plug splitting into small droplets. Typically, the previously reported methods are based on generating combinations of reagents or concentration gradients prior to droplet production. Our picoinjection methodology is complementary to these systems since combinations of reagents are added only after droplet formation, which enables to test concentration gradients of reagents on cells or reactions that require a preceding droplet incubation step. Applications of interest might include the study of components that affect hyphae in filamentous fungi, which first need to be incubated to allow hyphal growth(47), to optimize assay component concentrations for the detection of secreted cell products such as cytokines or antibodies(48), to find the optimal concentration of a component in multistep chemical synthesis(29), or other, multistep protocols. Although combinations of reagents can also be added to incubated droplets by fusing them with preformed droplet libraries(15), our method provides a higher degree of flexibility since for example the length of the concentration sweep can be adjusted (e.g. from 30 s to 10 min), and the added droplet volumes are accurately tunable within an experiment.

Conclusions

We demonstrated a novel method for robust serial picoinjection with high flexibility based on combined pressure and flow rate control. Controlling the flow rate of an injector allowed for highly accurate reagent addition of predefined volumes, while setting the calibrated equilibrium pressure enabled to turn off individual injectors. We illustrated the strength of this method for 1, 2 and 3 picoinjectors, for both picoinjection with time-invariant and time-variant settings, and hereby showed an unprecedented picoinjection versatility. We furthermore demonstrated the potential of the serial picoinjection technology for fast compound concentration screenings. Besides the proof-of-concepts performed in this work, many other combinations of injector conditions can be established using the developed methodology. Therefore, we anticipate that the methods described in this work will inspire researchers and lead to a wider adaptation of the impactful serial picoinjection technology.

Author Contributions

J.B. : conceived and planned experiments, carried out experiments and performed data analysis, wrote manuscript. H.O.d.B.: carried out experiments and performed analysis, revised manuscript. I.R.: contribution to hardware and software tools, revised manuscript. M.L.F.: cell line generation, revised manuscript. S.E.: cell line generation, project funding, revised manuscript. J.L.: project funding, discussion experimental concepts and data analysis, revised manuscript.

Conflicts of interest

There are no conflicts to declare.

Acknowledgements

This work has received funding from Research Foundation Flanders (11A1719N, G042918N, G090120) and the KU Leuven (IDN/20/011; C24E/20/035).

References

1. Zilionis R, Nainys J, Veres A, Savova V, Zemmour D, Klein AM, et al. Single-cell barcoding and sequencing using droplet microfluidics. Nat Protoc. 2017;12(1):44–73.
2. Ng EX, Miller MA, Jing T, Lauffenburger DA, Chen CH. Low-volume multiplexed proteolytic activity assay and inhibitor analysis through a pico-injector array. Lab Chip. 2015;15(4):1153–9.
3. Davie K, Janssens J, Koldere D, De Waegeneer M, Pech U, Kreft Ł, et al. A single-cell transcriptome atlas of the aging drosophila brain. Cell. 2018;174(4):982–98.
4. Autour A, Ryckelynck M. Ultrahigh-throughput improvement and discovery of enzymes using droplet-based microfluidic screening. Micromachines. 2017;8(4):128.
5. Holstein JM, Gylstorff C, Hollfelder F. Cell-free directed evolution of a protease in microdroplets at ultrahigh throughput. ACS Synth Biol. 2021;10(2):252–7.
6. Macosko EZ, Basu A, Satija R, Nemesh J, Shekhar K, Goldman M, et al. Highly parallel genome-wide expression profiling of individual cells using nanoliter droplets. Cell. 2015;161(5):1202–14.
7. Mazutis L, Griffiths AD. Preparation of monodisperse emulsions by hydrodynamic size fractionation. Appl Phys Lett. 2009;95(20):204103.
8. Gérard A, Jensen A, Griffiths AD, Bruhns P, Brenan C, Woolfe A, et al. High-throughput single-cell activity-based screening and sequencing of antibodies using droplet microfluidics. Nat Biotechnol. 2020;38:715–721.
9. Shim JU, Ranasinghe RT, Smith CA, Ibrahim SM, Hollfelder F, Huck WTS, et al. Ultrarapid generation of femtoliter microfluidic droplets for single-molecule-counting immunoassays. ACS Nano. 2013;7(7):5955–64.
10. Joensson HN, Andersson Svahn H. Droplet microfluidics - A tool for single-cell analysis. Angew Chemie - Int Ed. 2012;51(49):12176–92.
11. Mazutis L, Gilbert J, Ung WL, Weitz DA, Griffiths AD, Heyman JA. Single-cell analysis and sorting using droplet-based microfluidics. Nat Protoc. 2013;8(5):870–91.
12. Li P, Ma Z, Zhou Y, Collins DJ, Wang Z, Ai Y. Detachable acoustophoretic system for fluorescence-activated sorting at the single-droplet Level. Anal Chem. 2019;91(15):9970–7.
13. Verbruggen B, Tóth T, Cornaglia M, Puers R, Gijs MAM, Lammertyn J. Separation of magnetic microparticles in segmented flow using asymmetric splitting regimes.

Microfluid Nanofluidics. 2014;18(1):91–102.
14. Link DR, Anna SL, Weitz DA, Stone HA. Geometrically mediated breakup of drops in microfluidic devices. Phys Rev Lett. 2004;92(5):054503.
15. Theberge AB, Mayot E, El Harrak A, Kleinschmidt F, Huck WTS, Griffiths AD. Microfluidic platform for combinatorial synthesis in picolitre droplets. Lab Chip. 2012;12(7):1320–6.
16. Mazutis L, Baret J-C, Griffiths AD. A fast and efficient microfluidic system for highly selective one-to-one droplet fusion. Lab Chip. 2009;9(18):2665–72.
17. Abate AR, Hung T, Mary P, Agresti JJ, Weitz DA. High-throughput injection with microfluidics using picoinjectors. Proc Natl Acad Sci. 2010;107(45):19163–6.
18. Rhee M, Light YK, Yilmaz S, Adams PD, Saxena D, Meagher RJ, et al. Pressure stabilizer for reproducible picoinjection in droplet microfluidic systems. Lab Chip. 2014;14(23):4533–9.
19. Beneyton T, Coldren F, Baret JC, Griffiths AD, Taly V. CotA laccase: high-throughput manipulation and analysis of recombinant enzyme libraries expressed in E. coli using droplet-based microfluidics. Analyst. 2014;139(13):3314–23.
20. Ryckelynck M, Baudrey S, Rick C, Marin A, Coldren F, Westhof E, et al. Using droplet-based microfluidics to improve the catalytic properties of RNA under multiple-turnover conditions. RNA. 2015;21(3):458–69.
21. Chen CH, Miller MA, Sarkar A, Beste MT, Isaacson KB, Lauffenburger DA, et al. Multiplexed protease activity assay for low-volume clinical samples using droplet-based microfluidics and its application to endometriosis. J Am Chem Soc. 2013;135(5):1645–8.
22. Sjostrom SL, Joensson HN, Svahn HA. Multiplex analysis of enzyme kinetics and inhibition by droplet microfluidics using picoinjectors. Lab Chip. 2013;13(9):1754–61.
23. Abalde-Cela S, Gould A, Liu X, Kazamia E, Smith AG, Abell C. High-throughput detection of ethanol-producing cyanobacteria in a microdroplet platform. J R Soc Interface. 2015;12(106):0216.
24. Qiao Y, Zhao X, Zhu J, Tu R, Dong L, Wang L, et al. Fluorescence-activated droplet sorting of lipolytic microorganisms using a compact optical system. Lab Chip. 2018;18(1):190–6.
25. Qiao Y, Hu R, Chen D, Wang Z, Yu H, Fu Y, et al. Fluorescence-activated droplet sorting of PET degrading microorganisms. J Hazard Mater. 2022;424:127417.
26. Hammar P, Angermayr SA, Sjostrom SL, Van Der Meer J, Hellingwerf KJ, Hudson EP, et al. Single-cell screening of photosynthetic growth and lactate production by cyanobacteria. Biotechnol Biofuels. 2015;8(1):193.
27. Eastburn DJ, Sciambi A, Abate AR. Ultrahigh-throughput mammalian single-cell reverse-transcriptase polymerase chain reaction in microfluidic drops. Anal Chem. 2013;85(16):8016–21.
28. Li S, Zeng M, Gaule T, McPherson MJ, Meldrum FC. Passive picoinjection enables controlled crystallization in a droplet microfluidic device. Small. 2017;13(41):1702154.
29. Yuan H, Pan Y, Tian J, Chao Y, Li J, Shum HC. Electricity-free picoinjection assisted droplet microfluidics. Sensors Actuators, B Chem. 2019;298:126766.
30. Ahmed H, Stokke BT. Fabrication of monodisperse alginate microgel beads by microfluidic picoinjection: A chelate free approach. Lab Chip. 2021;21(11):2232–43.
31. Karimi M, Jacobs TB. GoldenGateway: A DNA assembly method for plant biotechnology. Trends Plant Sci. 2021;26(1):95–6.
32. Sciambi A, Abate AR. Generating electric fields in PDMS microfluidic devices with salt water electrodes. Lab Chip. 2014;14(15):2605–9.
33. Fluigent. Software Development Kit [Internet]. [cited 2022 Feb 21]. Available from: https://www.fluigent.com/research/software-solutions/software-development-kit/
34. Bingham NH., Fry JM. Adding additional covariates and the analysis of covariance. In: Regression: Linear models in statistics. 2010. p. 129–48.
35. Mathworks. Analysis of covariance [Internet]. [cited 2022 Mar 6]. Available from: https://nl.mathworks.com/help/stats/analysis-of-covariance.html
36. SeeedStudio. Grove - 4-Channel SPDT Relay [Internet]. [cited 2022 Jun 10]. Available from: https://www.seeedstudio.com/Grove-4-Channel-SPDT-Relay-p-3119.html
37. Stoltzfus JC. Logistic regression: A brief primer. Acad Emerg Med. 2011;18(10):1099–104.
38. Klimberg R, McCullough BD. Fundamentals of predictive analytics with JMP [Internet]. 2013 [cited 2022 Jun 10]. p. 292. Available from: https://support.sas.com/publishing/pubcat/chaps/64395.pdfefpO4Xm9gTun4CwCA&ved=0CEkQ6AEwAw#v=onepage&q=hidden nodes sample size&f=false
39. Fluigent. DFC, “self-learning” flow rate control algorithm [Internet]. [cited 2022 Feb 21]. Available from: https://www.fluigent.com/resources-support/expertise/expertise-reviews/advantages-of-pressure-based-microfluidics/dfc-self-learning-flow-rate-control-algorithm/?nowprocket=1
40. Churski K, Kaminski TS, Jakiela S, Kamysz W, Baranska-Rybak W, Weibel DB, et al. Rapid screening of antibiotic toxicity in an automated microdroplet system. Lab Chip. 2012;12(9):1629–37.
41. Cao J, Kürsten D, Schneider S, Knauer A, Günther PM, Köhler JM. Uncovering toxicological complexity by multi-dimensional screenings in microsegmented flow: Modulation of antibiotic interference by nanoparticles. Lab Chip. 2012;12(3):474–84.
42. Bui MPN, Li CA, Han KN, Choo J, Lee EK, Seong GH. Enzyme kinetic measurements using a droplet-based microfluidic system with a concentration gradient. Anal Chem. 2011;83(5):1603–8.
43. Kielpinski M, Walther O, Cao J, Henkel T, Köhler JM, Groß GA. Microfluidic chamber design for controlled droplet expansion and coalescence. Micromachines. 2020;11(4):394.
44. Zaremba D, Blonski S, Korczyk PM. Concentration on

demand – A microfluidic system for precise adjustment of the content of single droplets. Chem Eng J. 2022;430:132935.

45. Zhang P, Kaushik A, Hsieh K, Wang TH. Customizing droplet contents and dynamic ranges via integrated programmable picodroplet assembler. Microsystems Nanoeng. 2019;5:22.
46. Kaminski TS, Jakiela S, Czekalska MA, Postek W, Garstecki P. Automated generation of libraries of nL droplets. Lab Chip. 2012;12(20):3995–4002.
47. Iftikhar S, Vigne A, Sepulveda-Diaz JE. Droplet-based microfluidics platform for antifungal analysis against filamentous fungi. Sci Rep. 2021;11(1):22998.
48. Debs BE, Utharala R, Balyasnikova I V., Griffiths AD, Merten CA. Functional single-cell hybridoma screening using droplet-based microfluidics. Proc Natl Acad Sci. 2012;109(29):11570–5.